Climate Change Impacts on U.S. Electricity Demand: Insights from Micro-Consistent Aggregation of a Structural Model

Bentley Coffey[1] Ian Sue Wing[2] Ari Stern[2]

[1]Duke University

[2]Boston University

2015 International Energy Workshop

Plan of Talk

Climate Change and Energy Demand

- Concern over climate change has led to a sizeable empirical literature documenting the influence of temperature on a variety of economic outcomes (Dell et al, 2014b)
- Electric power is a particularly exposed sector, with more (less) extreme summer (winter) temperatures resulting in larger (smaller) cooling loads, and concomitant changes in electricity demand
- Since the late 1970s average U.S. temperatures have risen 0.31-0.48°F per decade, a trend which is expected to continue as the climate changes. Coincident net residential electricity use is expected to grow, with increased electricity demands for cooling outstripping savings from lower electricity demands due to reduced need for heating (Dell et al, 2014a)
- Previous research focused on how climate change affects *total* electric power
  - e.g. annual residential energy demand (Deschenes and Greenstone, 2011), or monthly electricity use (Aroonruengsawat and Auffhammer, 2011; Auffhammer and Aroonruengsawat, 2011)
- Because climate change increases the occurrence of heat waves (Kharin et al, 2013; Peterson et al, 2013; Herring et al, 2014; Kodra and Ganguly, 2014), the focus of GENCOs, TRANSCOs and ISOs/RTOs is on *maximum* load
- Peak demand occurs during the very hottest hours, driven by AC—53% of total demand and 65% of peak demand on extreme hot days in Phoenix (Salamanca et al, 2013), 20-33% of Madrid's July 19, 2008 peak (Izquierdo et al, 2011). During extremes peak units drive electricity costs 6× higher than average (Monitoring Analytics, 2013; Allcott, 2013), and threaten grid stability.

What We Do

- **Question: how strongly does instantaneous AC-driven electricity demand respond to heatwaves that portend increasing extreme summer temperatures—whose duration is on the scale of hours?**
- We develop a novel thermodynamically micro-founded model of electricity demand
- Perform econometric estimations on a unique high-frequency dataset of 2.3 million observations of hourly electric load over the period 2001-2012 for three power pools that account for 17% of U.S. electricity consumption
- We estimate per capita demand for electricity as a function of temperature and humidity within "weather" zones of service territories of three ISOs: the Electric Reliability Council of Texas (ERCOT), New York ISO (NYISO) and ISO New England (ISO-NE)

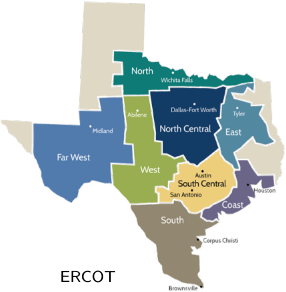

ERCOT

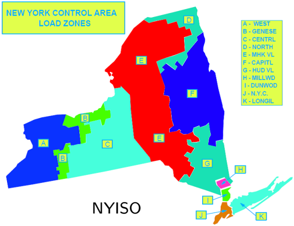

NYISO

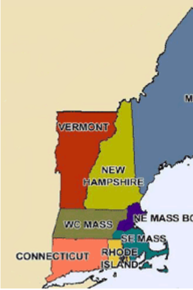

ISO-NE

Structural Model (I): Electricity Demand and Weather

i individuals, each with electricity demand q_i, divided into a "necessary" electricity consumed for HVAC, w_i, and discretionary electricity consumed out of residual disposable income after purchasing other necessary goods, g:

$$q_i = \gamma_i + w_i + \frac{\sigma}{p_E}\left(\mathscr{I}_i - p_E\left(\vartheta_i + w_i\right) - \sum_{g \neq E} p_g y_g\right) \tag{1}$$

$\mathscr{I}$ = total income, σ = discretionary electricity's share of disposable income, p_E, p_g = prices of electricity and other goods, y_g = necessary other goods consumption

Individuals have identical preferences for thermal comfort, defined by an ideal temperature and humidity (T^*, H^*). To maintain environmental equilibrium at (T^*, H^*) buildings' climate control systems transfer enthalpy (e, sensible heat + latent heat associated with phase changes in moisture) gained during each hour. Enthalphy gain/loss has four components:
Internal: Heat release by the human body and electrical appliances, which HVAC engineering calculations assume generates +6°F offset ($\mathcal{O}$) in indoor temperature relative to the standard 65°F degree day/HVAC setpoint threshold. Henceforth we assume that $T^* = 71$°F.
Conduction: $\propto$ differential between i's ambient temperature (T_i) and ideal temperature
Convection: Sensible and latent heat transmission via duct/door/window air movement, $\propto$ ambient temperature and humidity (H_i) differentials from ideals
Radiation: Energy gain from insolation, dependent on location on Earth's surface, axial tilt and its precession, eccentricity of orbit, (absolute) solar time, atmospheric conditions

Structural Model (II): Enthalpy Transfer

Internal enthalphy (assumed constant): $\dot{e}_i^{\text{Internal}} = \iota$

Conduction (Fourier's Law): $\dot{e}_i^{\text{Conduction}} = \kappa_i^{\text{Conduction}} \left(T_i - T^* \right)$ (2)

κ = ratio of building surface area to thermal resistance

Convection (Newton's Law)

$$\dot{e}_i^{\text{Convection}} = \kappa_i^{\text{Convection}} \left[\underbrace{\chi_{pa}(T_i - T^*)}_{\text{Sensible Heat}} + \underbrace{\chi_{ev}(H_i - H^*) + \chi_{pv}(T_i \; H_i - T^* H^*)}_{\text{Latent Heat}} \right] \tag{3}$$

χ_{pa}, χ_{pv} = specific heat capacities of dry air and water vapor; χ_{ve} = latent heat of evaporation of water

Radiation: $\dot{e}_i^{\text{Radiation}} \propto \kappa_i^{\text{Radiation}} \cdot \Psi[x_i, y_i, t_i^{\text{Clock}}, d]$ (4)

(x_i, y_i) and t^{Clock} = individual's grid coordinates and wall-clock time, d = day in the Julian calendar year. Ψ = a complex reduced-form clear-sky insolation function

Enthalpy transfer depends on the temperature ranges governed by the HVAC mode, $m = \{H \text{ (heating) }, V \text{ (ventilation) }, C \text{ (cooling) }\}$:

$$\dot{e}_{i,m} = \begin{cases} -(\dot{e}_i^{\text{Conduction}} + \dot{e}_i^{\text{Convection}} + \dot{e}_i^{\text{Radiation}} + \dot{e}_i^{\text{Internal}}) & T_i \in (-\infty, T^* - \mathcal{O}] \quad m = H \\ \dot{e}_i^{\text{Conduction}} + \dot{e}_i^{\text{Convection}} + \dot{e}_i^{\text{Radiation}} + \dot{e}_i^{\text{Internal}} & T_i \in (T^* - \mathcal{O}, T^*) \quad m = V \\ \dot{e}_i^{\text{Conduction}} + \dot{e}_i^{\text{Convection}} + \dot{e}_i^{\text{Radiation}} + \dot{e}_i^{\text{Internal}} & T_i \in [T^*, +\infty) \quad m = C \end{cases} \tag{5}$$

Insolation: Maine (ISO-NE/ME) vs. Texas Far West (ERCOT/FARWEST)

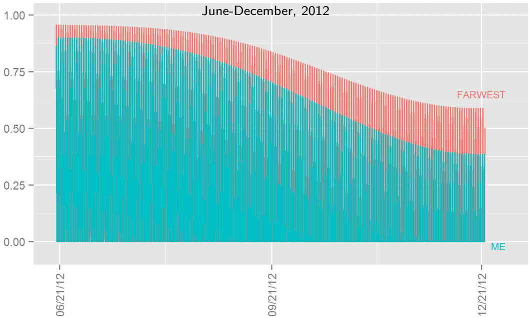

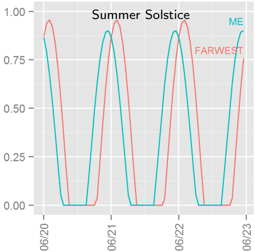

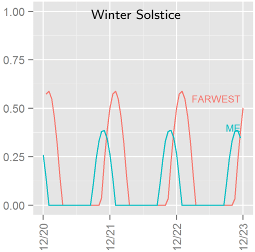

A Structural Model (III): From Enthalpy To Electricity Demand

Electricity necessary to perform the work associated with enthalpy transfer $\propto$ the coefficient of performance (CoP), which is bounded thermodynamically to a fraction, η, of the Carnot limit:

$$w_{i,m} = \frac{\dot{e}_{i,m}}{CoP_{i,m}} = \frac{\dot{e}_{i,m}}{\eta_{i.m}} \frac{\| T_i - T^* \|}{T^*} \tag{6}$$

Combining this with eqs. (2)-(5) yields a weather demand function that is quadratic in the ambient outdoor temperature (given humidity) and linear in humidity (given temperature):

$$\begin{aligned} w_{i,m} = & \underbrace{\frac{\kappa_i^{\text{Conduction}}}{\eta_{i,m} T^*} \| T_i - T^* \| (T_i - T^*) \cdot \delta_{i,m}}_{\text{Conduction}} + \underbrace{\chi_{pa} \frac{\kappa_i^{\text{Convection}}}{\eta_{i,m} T^*} \| T_i - T^* \| (T_i - T^*) \cdot \delta_{i,m}}_{\text{Convection: Sensible Heat}} \\ & + \underbrace{\frac{\kappa_i^{\text{Convection}}}{\eta_{i,m} T^*} \| T_i - T^* \| \{ \chi_{ev} (H_i - H^*) \cdot \delta_{i,m} + \chi_{pv} (T_i \; H_i - T^* H^*) \cdot \delta_{i,m} \}}_{\text{Convection: Latent Heat}} \\ & + \underbrace{\frac{\kappa_i^{\text{Radiation}}}{\eta_{i,m} T^*} \| T_i - T^* \| \Psi[x_i, y_i, t] \cdot \delta_{i,m}}_{\text{Radiation}} + \underbrace{\frac{\iota}{\eta_{i,m} T^*} \| T_i - T^* \| \cdot \delta_{i,m}}_{\text{Internal Heat Gain}} \end{aligned} \tag{7}$$

where $\delta_{i,m}$ = an indicator function which takes the value -1 in heating mode, and +1 otherwise

Individual Electricity Demand Response Function

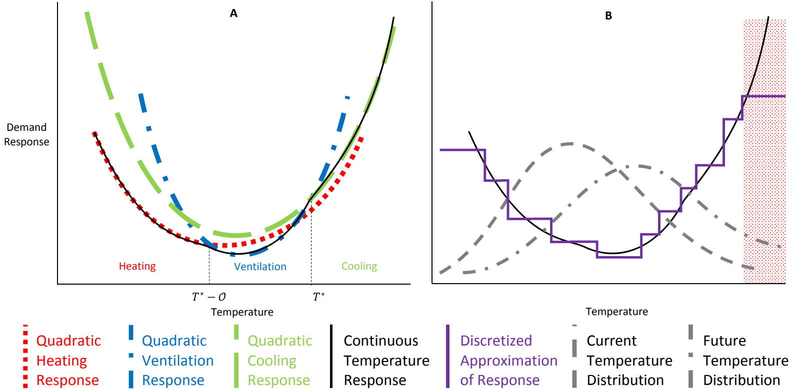

Black curve = eq. (7), purple step function = U-shaped profile in impacts literature:

$$w = \text{Fixed effects} + \text{Time effects} + \sum_b \rho_b\, \mathcal{C}[T \in (\underline{T}_b, \overline{T}_b)] + \text{Controls} + u \qquad (8)$$

$(\underline{T}_b, \overline{T}_b)$ = b^{th} temperature interval's boundaries, $\mathcal{C}$ = time exposure where T lies in each bin, ρ_b = constant bin-wise marginal effects

Micro-Consistent Aggregation (I)

We must consistently aggregate eq. (1) up to the level at which we observe electricity demand: the groups of counties that make up each ISO/RTO's weather zones, z. Summing across individuals within zones and dividing by zonal population (N_z) yields:

$$Q_z = \widetilde{Q}_z / N_z = \Gamma_z + W_z + \sigma \left(\frac{\mathscr{I}_z}{p_E} \right) + \Upsilon_z \left(\frac{-1}{p_E} \right) \tag{9}$$

Γ = non-weather related price-invariant per capita expenditure on other electricity, which can be specified as a time-dependent function

Eq. (7)'s individual-level parameters vary with unobserved, heterogeneous built environment attributes (buildings' surface area/volume, insulation R-factors, HVAC efficiency). But at any hour large numbers of individuals over wide geographic areas will experience the same ambient temperature and humidity, allowing us to group individuals in each zone into $j \in J_z$ building categories at $k \in K_z$ locations with $j \times k$ archetypical patterns of HVAC electricity use:

$$w^{\ddagger}_{j,k,m} = w_i \big|_{\kappa_i = \kappa_j, \eta_{i,m} = \eta_{j,m}, T_i = T_k, H_i = H_k, \delta_{i,m} = \delta_{k,m} = \delta[T_k \in (\underline{T}_m, \overline{T}_m)]} \tag{10}$$

With information on the distribution of population across locations and building types ($n^{\ddagger}_{j,k}$) per capita HVAC electricity use is easily calculated as the weighted sum

$$W_z = \sum_{j=1}^{J_z} \sum_{k=1}^{K_z} \sum_{m} \phi_{j,k} w^{\ddagger}_{j,k,m} \tag{11}$$

with weights $\phi_{j,k} = n^{\ddagger}_{j,k} / N_z$

Micro-Consistent Aggregation (II)

To take (11) to the data we rearrange terms and aggregate parameters into a vector of seven mode-specific unknown coefficients plus a constant, $\boldsymbol{\omega}$:

$$
\begin{aligned}
W_z = \sum_{j=1}^{J_z} \Bigg[& \sum_m \omega_{j,m}^{T} \left(\textstyle\sum_{k=1}^{K_z} \phi_{j,k} T_k \cdot \delta_{k,m} \right) + \sum_m \omega_{j,m}^{TT} \left(\textstyle\sum_{k=1}^{K_z} \phi_{j,k} T_k^2 \cdot \delta_{k,m} \right) \\
& + \sum_m \omega_{j,m}^{TH} \left(\textstyle\sum_{k=1}^{K_z} \phi_{j,k} T_k H_k \cdot \delta_{k,m} \right) + \sum_m \omega_{j,m}^{TTH} \left(\textstyle\sum_{k=1}^{K_z} \phi_{j,k} T_k^2 H_k \cdot \delta_{k,m} \right) \\
& + \sum_m \omega_{j,m}^{\Psi} \left(\textstyle\sum_{k=1}^{K_z} \phi_{j,k} \Psi_k \cdot \delta_{k,m} \right) + \sum_m \omega_{j,m}^{T\Psi} \left(\textstyle\sum_{k=1}^{K_z} \phi_{j,k} T_k \Psi_k \cdot \delta_{k,m} \right) \\
& + \sum_m \omega_{j,m}^{H} \left(\textstyle\sum_{k=1}^{K_z} \phi_{j,k} H_k \cdot \delta_{k,m} \right) \Bigg] + \omega_z^0
\end{aligned} \tag{12}
$$

Our aggregation procedure turns on the crucial othogonal decomposition

$$\omega_{j,m} = \beta_m + \xi_j \tag{13}$$

where $\beta =$ a systematic population-average component, $\xi =$ a random component that depends unobserved building characteristics. Taking expectations allows us to integrate out the latter.

Micro-Consistent Aggregation (III)

Our final reduced-form specification, given below, is estimated using OLS on a panel of hourly electricity load and weather data across z zones:

$$Q_{z,t} = \lambda_z + \text{Hour of Day}[t] + \text{Day of Week}[t] + \text{Year}\times\text{Month}[t] + \mathbb{E}[W]_{z,t} + \varepsilon \tag{14a}$$

where

$$\begin{aligned}\mathbb{E}[W]_z = \sum_m \Big[&\beta_m^T \left(\textstyle\sum_{k=1}^{K_z} \Phi_k T_k \cdot \delta_{k,m}\right) + \beta_m^{TT} \left(\textstyle\sum_{k=1}^{K_z} \Phi_k T_k^2 \cdot \delta_{k,m}\right) \\ &+ \beta_m^{TH} \left(\textstyle\sum_{k=1}^{K_z} \Phi_k T_k H_k \cdot \delta_{k,m}\right) + \beta_m^{TTH} \left(\textstyle\sum_{k=1}^{K_z} \Phi_k T_k^2 H_k \cdot \delta_{k,m}\right) \\ &+ \beta_m^{\Psi} \left(\textstyle\sum_{k=1}^{K_z} \Phi_k \Psi_k \cdot \delta_{k,m}\right) + \beta_m^{T\Psi} \left(\textstyle\sum_{k=1}^{K_z} \Phi_k T_k \Psi_k \cdot \delta_{k,m}\right) \\ &+ \beta_m^{H} \left(\textstyle\sum_{k=1}^{K_z} \Phi_k H_k \cdot \delta_{k,m}\right)\Big] + \beta_z^0\end{aligned} \tag{14b}$$

with weights $\Phi_k = \sum_j n^{\ddagger}_{j,k}/N_z$,
and setpoints $\underline{T}_H = \overline{T}_V = 65^\circ$F, $\underline{T}_C = \overline{T}_V = 71^\circ$F, $\underline{T}_H = -\infty$, $\overline{T}_C = +\infty$

Data (I): Electric Load

Zone	Number of Counties	Annual Population (millions) %-tiles: 25th	50th	75th	Load (GWh) %-tiles: 25th	50th	75th
Electric Reliability Council of Texas (ERCOT) 4/16/2003 [13:00]-12/31/12 [23:00] (85,019 hours)							
Coast	12	5.330	5.772	6.044	8.517	9.584	11.480
East	20	0.992	1.035	1.063	1.224	1.422	1.712
Far West	22	0.396	0.417	0.429	1.061	1.168	1.333
North	27	0.494	0.496	0.497	0.784	0.906	1.082
North Central	33	6.674	7.153	7.420	9.714	11.171	13.723
South Central	25	3.591	3.942	4.129	4.707	5.455	6.688
Southern	26	2.075	2.185	2.265	2.328	2.730	3.328
West	29	0.548	0.558	0.568	0.845	0.953	1.120
New York ISO (NYISO) 1/1/2002 [0:00]-12/31/2012 [23:00]* (96,319 hours)							
Capitl	13	1.253	1.268	1.275	1.123	1.306	1.459
Centrl	16	1.611	1.613	1.619	1.673	1.899	2.094
Dunwod	1	0.933	0.936	0.951	0.576	0.691	0.785
Genese	7	1.168	1.171	1.176	0.976	1.149	1.274
Hud Vl	10	2.661	2.676	2.710	1.016	1.172	1.317
Mhk Vl	18	2.069	2.080	2.082	0.735	0.868	0.983
Millwd	1	0.933	0.936	0.951	0.235	0.295	0.357
NYC/LongIl*	7	10.860	10.868	10.879	6.975	8.382	9.348
North	5	0.289	0.290	0.290	0.625	0.711	0.763
West	11	2.461	2.463	2.483	1.612	1.823	2.011
ISO New England (ISO-NE) 3/1/2003 [0:00]-12/31/12 [23:00] (86,256 hours)							
CT	8	3.507	3.546	3.577	3.129	3.711	4.186
ME	16	1.319	1.328	1.329	1.134	1.343	1.467
NE Mass Bost	4	3.533	3.575	3.649	2.520	2.967	3.283
NH	10	1.298	1.316	1.317	1.108	1.348	1.496
RI	5	1.053	1.055	1.068	0.793	0.948	1.060
SE Mass	5	1.279	1.281	1.288	1.458	1.746	1.957
VT	14	0.621	0.624	0.626	0.591	0.694	0.764
WC Mass	5	1.602	1.613	1.626	1.765	2.082	2.321

* The NYC/LongIl series stops at 1/30/2005 (23:00) and only has 26,892 observations

Data (II): Weather Covariates

North American Land Data Assimilation System (NLDAS-2) forcing files, recording T and H on a $1/8^\circ$ raster grid at an hourly time-step over the coterminous U.S., bilinearly interpolated to county polygons

	Heating[a,d]		Ventilation[b,d]		Cooling[c,d]	
	Mean	S.D.	Mean	S.D.	Mean	S.D.
	ERCOT					
$T \times 10^{-1}$	28.18	0.49	29.3	0.07	30.29	0.42
$T^2 \times 10^{-2}$	794.6	27.56	858.6	3.964	917.6	25.44
$T \times H \times 10^{-2}$	13.9	6.61	33.35	8.52	42.17	10.26
$T^2 \times H \times 10^{-3}$	394.1	192.1	977.4	250	1277	307.9
$\Psi \times 10$	1.48	2.40	2.32	3.04	3.62	3.62
$T \times \Psi$	41.91	68.08	67.97	89.15	109.8	110
Share of hours (%)[d]	27.10		1.70		39.50	
	NYISO					
$T \times 10^{-1}$	27.73	0.78	29.31	0.1	29.89	0.23
$T^2 \times 10^{-2}$	769.7	42.83	859.3	5.88	893.5	13.58
$T \times H \times 10^{-2}$	13.2	7.363	34.8	6.053	44.25	7.18
$T^2 \times H \times 10^{-3}$	371.3	215.6	1020	178.7	1324	220
$\Psi \times 10$	1.753	2.5	2.80	3.27	4.48	3.38
$T \times \Psi$	48.98	70.28	82.17	96.01	13	101.1
Share of hours (%)[d]	70.30		4.70		7.70	
	ISO-NE					
$T \times 10^{-1}$	27.79	0.75	29.31	0.081	29.92	0.21
$T^2 \times 10^{-2}$	772.6	41.57	859	4.736	895.4	12.36
$T \times H \times 10^{-2}$	13.59	7.54	36.26	5.6	44.74	7.09
$T^2 \times H \times 10^{-3}$	382.9	220.4	1063	165	1339	215.8
$\Psi \times 10$	1.786	2.53	2.86	3.26	4.58	3.33
$T \times \Psi$	50.03	71.33	83.71	95.54	136.9	99.46
Share of hours (%)[d]	71.10		4.20		5.30	

[a] $T \leq 291$K ($\approx 64^\circ$F), [b] $291\text{K} < T < 295$K, [c] $295\text{K} \leq T$ ($\approx 72^\circ$F)

[d] Shares do not sum to 100% because these summary statistics are generated from the subset of observations where all zones are completely within a given HVAC mode. The difference represents hourly observations where different counties in each zone are in different HVAC modes, which is common in the shoulder seasons in northerly locations.

Temperature Impacts on Summer Per Capita Load

A. Diurnal Load Profiles (kW) by Average Daily Temperature

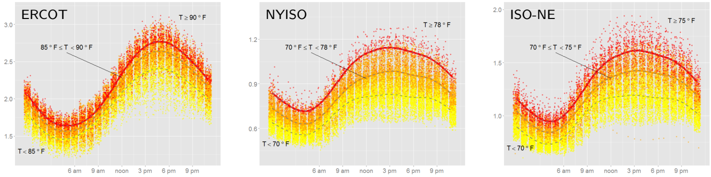

B. Hourly Per Capita Load (kW) by Population-Weighted Temperature

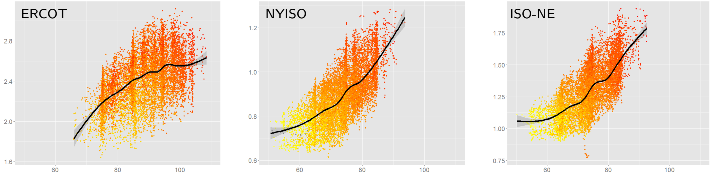

C. Relationship Between Maximum and Average Daily Temperatures (°F)

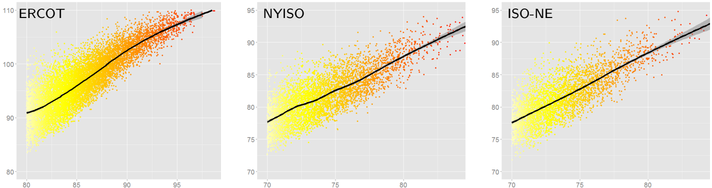

Estimated Demand Responses by ISO/RTO (I)

	ERCOT		NYISO		ISO-NE	
Heating						
T	-8019.0	(147.7)*	-1457.0	(22.7)*	-182.4	(23.6)
T^2	138.5	(2.6)*	25.8	(0.4)*	1.8	(0.4)
$T \times H$	-3797.0	(425.3)*	-4054.0	(73.0)*	-3136.0	(77.8)*
$T^2 \times H$	68.7	(7.4)*	70.7	(1.3)*	56.7	(1.4)*
Ψ	879.5	(11.1)*	113.4	(2.0)*	109.7	(2.2)*
$T \times \Psi$	-31.5	(0.4)*	-4.1	(0.1)*	-4.0	(0.1)*
H	52320.0	(6081.0)*	58160.0	(1048.0)*	43370.0	(1118.0)*
Ventilation						
T	-7800.0	(145.5)*	-1425.0	(30.1)*	-139.6	(31.1)
T^2	131.0	(2.7)*	24.6	(0.8)*	0.4	(0.8)
$T \times H$	-1624.0	(4277.0)	-4350.0	(1724.0)	253.9	(1863.0)
$T^2 \times H$	34.5	(72.9)	76.2	(29.3)	0.6	(31.7)
Ψ	621.5	(74.2)*	273.5	(28.2)*	347.8	(30.1)*
$T \times \Psi$	-22.6	(2.5)*	-9.7	(1.0)*	-12.3	(1.0)*
H	18040.0	(62750.0)	62120.0	(25340.0)	-7820.0	(27360.0)
Cooling						
T	-8207.0	(136.7)*	-1740.0	(22.0)*	-824.0	(23.1)*
T^2	144.8	(2.3)*	35.3	(0.4)*	23.5	(0.5)*
$T \times H$	3254.0	(130.7)*	-3533.0	(165.1)*	-6646.0	(200.9)*
$T^2 \times H$	-52.9	(2.2)*	58.0	(2.7)*	109.6	(3.3)*
Ψ	905.2	(7.4)*	288.3	(11.2)*	688.4	(13.1)*
$T \times \Psi$	-32.1	(0.2)*	-10.2	(0.4)*	-23.8	(0.4)*
H	-49820.0	(1972.0)*	53970.0	(2504.0)*	100900.0	(3044.0)*
Constant	11780.0	(2069)*	21460.0	(305.6)*	4579.0	(317.6)*
Adj. R-sq	0.85		0.95		0.91	
% of variation explained by:						
Weather covariates	0.50		0.07		0.24	
Fixed effects	0.73		0.93		0.84	
% of variation explained by Temperature and Humidity:						
Lower bound:	0.12		0.02		0.07	
Upper bound:	0.50		0.07		0.24	
N. Obs.	680,074		894,190		689,873	

Estimated Demand Responses by ISO/RTO

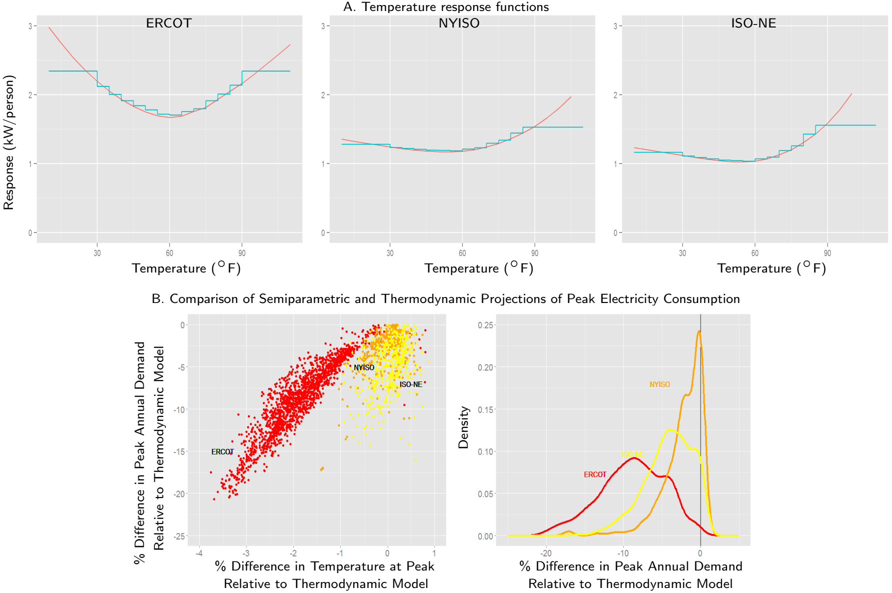

Climate Change Impacts: % Change in Average Total Electricity Consumption, 2081-2100 vs. 2021-2050

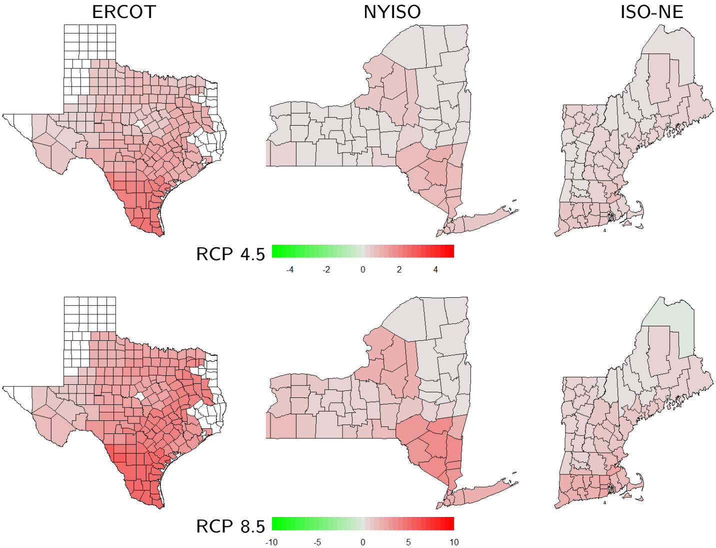

Climate Change Impacts: % Change in Average Peak Electricity Consumption, 2081-2100 vs. 2021-2050

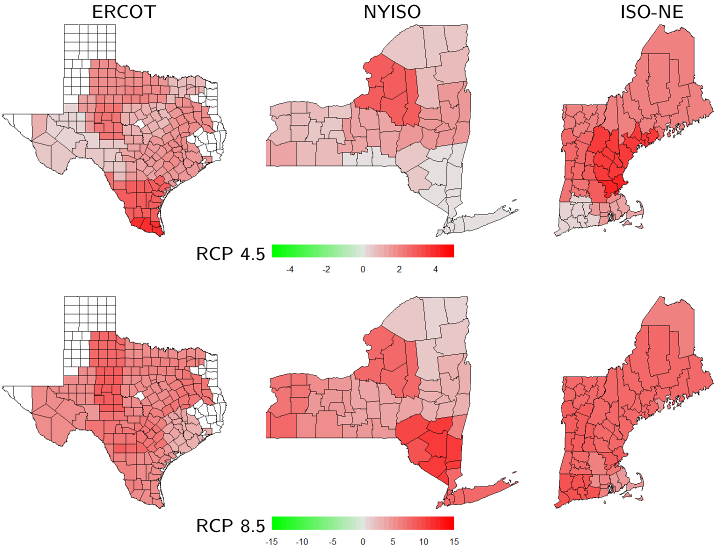

Caveats and Further Research

There are several caveats to these results, and we are addressing them:

Limited geographic coverage: Research is ongoing to estimate similar results for PJM, California ISO and Midwest ISO, and load and weather data are being gathered for additional major load-balancing authorities (SERC, FRCC, Southwest Power Pool), with the ultimate objective of generating estimates of demand response and impact for the entire coterminous U.S.

Exogenous assignment of weather exposure to heating/ventilation/cooling modes: Efforts are ongoing to endogenize this assignment via development and testing of maximum likelihood estimators

The character of heterogeneity assumed in eq. (13) **ignores potential systematic spatial trends in residential and commercial building characteristics that are likely correlated with building energy performance:** The way to address this is to exploit Census cross-tabulations of the distribution of population across housing unit densities and ages to develop more sophisticated weights in (14b). Relevant data are currently being explored.

Impact estimates are constructed using projections from a single ESM, and do not use the present climate as a baseline: ESM projections' finest temporal resolution is 3-hour averages, and it is well known that ESMs' internal variability underestimates natural variability. Thus, even with vigorous warming the upper tail of the distribution of present-day hourly temperatures can exceed that of the distribution of projected 3-hour average temperatures. Apples-to-apples comparison requires synthetic present-day baselines, constructed by combining our estimates with ESM simulations of current climate on a 3-hour time step. We plan to do this for several ESMs in the CMIP5 archive.

References I

Allcott, H. (2013). Real-Time Pricing and Electricity Market Design, Working Paper, NYU Economics Dept.

Aroonruengsawat A, Auffhammer M (2011) Impacts of climate change on residential electricity consumption: evidence from billing data, in G. Libecap and R.H. Steckel (eds.), The economics of climate change: past and present. University of Chicago Press.

Auffhammer, M. and A. Aroonruengsawat (2011). Simulating the Impacts of Climate Change, Prices and Population on California's Residential Electricity Consumption. Climatic Change 109(S1): 191-210.

Christensen, J.H., F. Boberg, O.B. Christensen, and P. Lucas-Picher (2008). On the need for bias correction of regional climate change projections of temperature and precipitation, Geophysical Research Letters 35: L20709.

Dell, M., B.F. Jones, and B.A. Olken (2014). What Do We Learn from the Weather? The New Climate-Economy Literature, Journal of Economic Literature 52(3): 740-798.

Dell, J., S. Tierney, G. Franco, R. G. Newell, R. Richels, J. Weyant, and T. J. Wilbanks (2014). Ch. 4: Energy Supply and Use. Climate Change Impacts in the United States: The Third National Climate Assessment, J. M. Melillo, Terese (T.C.) Richmond, and G. W. Yohe, Eds., U.S. Global Change Research Program, 113-129. doi:10.7930/J0BG2KWD

Deschenes O., and M. Greenstone (2011). Climate Change, Mortality, and Adaptation: Evidence from Annual Fluctuations in Weather in the US, American Economic Journal: Applied Economics, 3(4): 152-85.

Herring, S. C., M. P. Hoerling, T. C. Peterson, and P. A. Stott, (eds.) (2014). Explaining Extreme Events of 2013 from a Climate Perspective. Bulletin of the American Meteorological Society 95(9): S1S96.

Izquierdo, M., A. Moreno-Rodrguez, A. Gonzlez-Gil, N. Garca-Hernando (2011). Air conditioning in the region of Madrid, Spain: An approach to electricity consumption, economics and CO_2 emissions, Energy 36(3): 1630-1639.

Kharin, V.V., F.W. Zwiers, X. Zhang, and M. Wehner (2013). Changes in temperature and precipitation extremes in the CMIP5 ensemble, Climatic Change 119: 345-357.

Kodra, E. and A.R. Ganguly (2014). Asymmetry of projected increases in extreme temperature distributions, Scientific Reports 4: Art. no 5884 doi:10.1038/srep05884

Miller, R.L., G.A. Schmidt, L.S. Nazarenko, N. Tausnev, S.E. Bauer, A.D. Del Genio, M. Kelley, K.K. Lo, R. Ruedy, D.T. Shindell, I. Aleinov, M. Bauer, R. Bleck, V. Canuto, Y. Chen, Y. Cheng, T.L. Clune, G. Faluvegi, J.E. Hansen, R.J. Healy, N.Y. Kiang, D. Koch, A.A. Lacis, A.N. LeGrande, J. Lerner, S. Menon, V. Oinas, C. Perez Garca-Pando, J.P. Perlwitz, M.J. Puma, D. Rind, A. Romanou, G.L. Russell, Mki. Sato, S. Sun, K. Tsigaridis, N. Unger, A. Voulgarakis, M.-S. Yao, and J. Zhang, 2014: CMIP5 historical simulations (1850-2012) with GISS ModelE2, Journal of Advances in Modeling Earth Systems 6: 441-477.

References II

Mitchell, K.E., D. Lohmann, P. Houser, E.F. Wood, J.S. Schaake, A. Robock, B.A. Cosgrove, J. Sheffield, Q. Duan, L. Luo, W.R. Higgins, R.T. Pinker, J.D. Tarpley, D.P. Lettenmaier, C.H. Marshall, J.K. Entin, M. Pan, W. Shi, V. Koren, J. Meng, B.H. Ramsay, and A.A. Bailey (2004). The multi-institution North American Land Data Assimilation System (NLDAS): Utilizing multiple GCIP products and partners in a continental distributed hydrological modeling system, Journal of Geophysical Research: Atmospheres 109 D7: 2156-2202.

Monitoring Analytics (2013). 2012 State of the Market Report for PJM, http://www.monitoringanalytics.com/reports/PJM_State_of_the_Market/2012/2012-som-pjm-volume1.pdf

Peterson, T. C. et al. (2013). Monitoring and understanding changes in heat waves, cold waves, floods and droughts in the United States: State of knowledge, Bulletin of the American Meteorological Society 94: 821-834.

Salamanca, F., M. Georgescu, A. Mahalov, M. Moustaoui, M. Wang and B.M. Svoma (2013). Assessing summertime urban air conditioning consumption in a semiarid environment Environmental Research Letters 8: 034022 doi:10.1088/1748-9326/8/3/034022

Schmidt, G.A., M. Kelley, L. Nazarenko, R. Ruedy, G.L. Russell, I. Aleinov, M. Bauer, S.E. Bauer, M.K. Bhat, R. Bleck, V. Canuto, Y.-H. Chen, Y. Cheng, T.L. Clune, A. Del Genio, R. de Fainchtein, G. Faluvegi, J.E. Hansen, R.J. Healy, N.Y. Kiang, D. Koch, A.A. Lacis, A.N. LeGrande, J. Lerner, K.K. Lo, E.E. Matthews, S. Menon, R.L. Miller, V. Oinas, A.O. Oloso, J.P. Perlwitz, M.J. Puma, W.M. Putman, D. Rind, A. Romanou, Mki. Sato, D.T. Shindell, S. Sun, R.A. Syed, N. Tausnev, K. Tsigaridis, N. Unger, A. Voulgarakis, M.-S. Yao, and J. Zhang (2014). Configuration and assessment of the GISS ModelE2 contributions to the CMIP5 archive, Journal of Advances in Modeling Earth Systems 6: 141-184.

Taylor, K.E., R.J. Stouffer and G.A. Meehl (2012). An overview of CMIP5 and the experiment design, Bulletin of the American Meteorological Society 93(4): 485-498.

U.S. Energy Information Administration (2009). Residential Energy Consumption Survey, 2009, http://www.eia.gov/consumption/residential/index.cfm

Van Vuuren, D.P., J. Edmonds, M. Kainuma, K. Riahi, A. Thomson, K. Hibbard, G.C. Hurtt, T. Kram, V. Krey, J.-F. Lamarque, T. Masui, M. Meinshausen, N. Nakicenovic, S.J. Smith and S.K. Rose (2011). The representative concentration pathways: an overview, Climatic Change 109: 5-31.

Xia, Y., et al (2012). Continental-scale water and energy flux analysis and validation for the North American Land Data Assimilation System project phase 2 (NLDAS-2): 1. Intercomparison and application of model products, Journal of Geophysical Research: Atmospheres 117 D3: 2156-2202.